Ecological Indicators 133 (2021) 108390

Contents lists available at ScienceDirect

Ecological Indicators

journal homepage: www.elsevier.com/locate/ecolind

Original Articles

Assessment of the response of tropical dry forests to El Niño southern oscillation

Lidong Zou [a,b], Sen Cao [b,c], Zaichun Zhu [a,*], Arturo Sanchez-Azofeifa [b,*]

[a] School of Urban Planning and Design, Peking University Shenzhen Graduate School, Peking University, Shenzhen 518055, China
[b] Department of Earth and Atmospheric Sciences, University of Alberta, Edmonton T6G 2E3, Canada
[c] Key Laboratory for Geo-Environmental Monitoring of Coastal Zone of the Ministry of Natural Resources & Guangdong Key Laboratory of Urban Informatics & Shenzhen Key Laboratory of Spatial Smart Sensing and Services & Research Institute for Smart Cities, Shenzhen University, Shenzhen 518060, China

ARTICLE INFO

Keywords:
Tropical dry forests
VCI
TCI
ENSO
Drought

ABSTRACT

Tropical Dry Forests (TDFs) in the Americas are significantly affected by drought related to El Niño Southern Oscillation (ENSO). The analysis builds upon two drought indices: the MODIS-derived Vegetation Condition Index (VCI) and Temperature Condition Index (TCI) and the Sea Surface Temperature (SST) anomaly in the Niño 3.4 region. Temporal correlation analysis and Moving Window Correlation Analysis (MWCA) were used to explore the long-term and short-term responses at multiple sites. Results illustrate Gross Primary Productivity (GPP) at SRNP-EMSS (Santa Rosa National Park Environmental Monitoring Super Site) and PEMS (Parque Estadual da Mata Seca) in the dry season were negatively impacted by the long-term SST anomaly across multiple ENSO phases (warm, neutral, and cold phases), while there was no long-term impact at CCBR (Chamela-Cuixmala Biosphere Reserve) and TVMWR (Tucabaca Valley Municipal Wildlife Reserve). Findings from a short-term perspective, suggest that the GPP at SRNP-EMSS and CCBR were sensitive to the ENSO warm phase. TDFs GPP at PEMS and TVMWR were resistant to El Niño. Our results reveal that stronger El Niño events may lead to severe droughts in more regions across TDFs, but there is no direct relationship between the intensity of an individual El Niño event and the precipitation condition in each study site. Except for their teleconnections, the biophysical characteristics and seasonality can impact the response of ENSO on the GPP.

1. Introduction

Tropical Dry Forests (TDFs) are ecosystems dominated by deciduous species, with mean annual precipitation of 700–2000 mm, an average annual temperature greater than 25 °C, and a dry season between 4 and 6 months where the precipitation is less than 100 mm (Sanchez-Azofeifa et al., 2005).

Global climate models predict more severe droughts, in terms of magnitude and duration, in TDFs (Castro et al., 2018; Chadwick et al., 2016). TDFs are susceptible to droughts because the regimes of precipitation determine phenological patterns and water availability is the limiting factor for plant growth and regeneration (Castro et al., 2018; Lopezaraiza-Mikel et al., 2013). One important source of droughts is El Niño Southern Oscillation (ENSO) (Gregory et al., 2019). ENSO is defined as a coupled mechanism between large-scale oceanic and atmospheric circulation processes in the equatorial Pacific Ocean that affects global climate and weather (Juan et al., 2021). This mechanism leads to the redistribution of precipitation and temperature patterns for certain regions of the world (Cai et al., 2021). El Niño is the warm phase of ENSO resulting from a weakening of trade winds and warmer Sea Surface Temperature (SST) across the east and central tropical Pacific, while La Niña is the cold phase of ENSO associated with stronger trade winds and cooler SST (Cai et al., 2021).

El Niño-induced droughts are pronounced in central America and north and northeast of South America where massive TDFs are located (Castro et al., 2018; Holmgren et al., 2001; Zou et al., 2020a). Severe El Niño-induced drought can change the structure and function of the forest ecosystem, destroy biodiversity, increase the mortality rate, and cause wildfires (Allen et al., 2010; Browne et al., 2021; Fahad et al., 2019; 2021a). As such, the provision of ecosystem services is extremely affected (Fahad et al., 2021b).

Satellite remote sensing has been broadly used to identify terrestrial biospheric dynamics linked to El Niño due to its advantages of high temporal resolution and large and consistent coverage areas (Doughty

* Corresponding authors.
E-mail addresses: zhuzc@pkusz.edu.cn (Z. Zhu), gasanche@ualberta.ca (A. Sanchez-Azofeifa).

https://doi.org/10.1016/j.ecolind.2021.108390
Received 25 August 2021; Received in revised form 8 November 2021; Accepted 16 November 2021
Available online 23 November 2021
1470-160X/© 2021 The Authors. Published by Elsevier Ltd. This is an open access article under the CC BY-NC-ND license (http://creativecommons.org/licenses/by-nc-nd/4.0/).

et al., 2021). The satellite-derived Normalized Difference Vegetation Index (NDVI) is one of the most commonly used vegetation indices; it reflects greenness and vigor because it is highly correlated with green leaf density and chlorophyll content in plants (Piao et al., 2020). As a modified NDVI, the Enhanced Vegetation Index (EVI) has improved sensitivity for monitoring drought in high biomass regions such as Tropical Rainfall Forests (Doughty et al., 2021). Similarly, the indices derived from the combination of Near Infrared (NIR) and Shortwave Infrared (SWIR), for instance, Normalized Difference Water Index (NDWI) and Land Surface Water Index (LSWI) have been proven the sensitivity to capture the water content of vegetation (Bajgain et al., 2015; Sun et al., 2013). There exist uncertainties for estimating vegetation water content using NIR-SWIR indices when canopy density is low or has not reached ground closure. As a complement, Land Surface Temperature (LST) derived from Thermal Infrared (TIR) is a state parameter that is widely used in formulating the water and energy budget at the atmosphere-surface interface (Wan et al., 2020). It can be considered as a proxy for assessing the evapotranspiration and vegetation water stress (Wan et al., 2020). Remote sensing drought indices, such as the Vegetation Condition Index (VCI), Normalized Difference Drought Index and the Temperature Condition Index (TCI) have been derived using time series of remotely sensed parameters (NDVI NDWI, and LST) to monitor vegetation stress and the effects of El Niño on vegetation (Bajgain et al., 2015). These drought indices allow vegetation stress and the impacts of El Niño on vegetation to be compared in different ecosystems in various regions (Zhang et al. 2017).

Numerous studies have investigated the vulnerability and resistance of ecosystems to ENSO from a long-term perspective (Campos, 2018 ; Nagai et al., 2007). Mennis (2001) explored the relationship between the SST anomaly in Pacific Niño 3.4 and NDVI in the Southeast USA for the period 1982–1992. The result indicated that El Niño events triggered a decline in vegetation vigor, and the SST anomaly had the strongest correlation with the NDVI for deciduous forests and a weak correlation with the NDVI for evergreen forests and croplands. Nagai et al. (2007) examined the relationship among time-series NDVI, climate indices (precipitation, temperature, and incoming surface solar radiation), and ENSO proxy over tropical rainforests in the Amazon basin and southeastern Asia from 1981 to 2000. Precipitation and temperature affected by ENSO are more important factors in controlling vegetation activities over tropical rainforests than incoming surface solar radiation. The teleconnections between ENSO and climate variables (e.g. precipitation and temperature) were reported by Campos in Santa Rosa National Park, Costa Rica, where TDFs inhabit. The driest and wettest periods on record happened in connection with strong El Niño and La Niña, respectively (Campos, 2018).

On the other hand, a number of studies analyzed the ENSO-related impacts on various ecosystems in tropical regions (Castro et al., 2018; Doughty et al., 2021). Some previous studies investigated the short-term response of the vegetated surface to ENSO during an individual El Niño event (Anyamba et al., 2002; Boyd et al., 2002). However, such studies failed to assess the impacts of El Niño on ecosystems precisely because the El Niño-affected areas cannot be coherent between different El Niño events (Erasmi et al., 2009). For example, 2009/2010 ENSO-driven drought event mostly affected the western and southern Amazon Basin (Marengo et al., 2011), whereas the northern and southeastern regions were largely influenced by 2014/2016 ENSO-driven drought (Jiménez-Muñoz et al., 2016). To solve this problem, a Moving Window Correlation Analysis (MWCA) is more recently used to assess the teleconnection between El Niño and ecosystems based on multiple El Niño events (Erasmi et al., 2009;). For example, Erasmi et al. (2009) investigated El Niño-related impacts on various tropical ecosystems in Indonesia during the period 1982–2006, by analyzing the relationship between monthly ENSO proxies and NDVI based on a MWCA. They found that the resistance of vegetation to drought stress is strongly affected by land-use intensity, and degraded forest areas and croplands are more sensitive to drought conditions than natural forests; Propastin et al. (2010) analyzed the vulnerability of vegetated surfaces over Africa to El Niño using MWCA for the period 1982–2006. The impacts of El Niño on vegetation largely depend on the vegetation type, and wooded and non-wooded vegetation types are more sensitive than tropical rainforests. In addition, Castro et al. explored the impact of drought on the productivity of TDFs in Santa Rosa National Park, Costa Rica during the 2014–2016 El Niño event. They found that gross primary productivity declined by 13% and 42% during the 2014 and 2015 drought seasons, respectively (Castro et al., 2018). However, to our knowledge, no research on the teleconnection between ENSO signal and vegetation variability in TDFs has been published.

The objective of this study is to quantify the response of TDFs to ENSO from long-term and short-term perspectives at multiple sites across the Americas. We use time-series satellite-based VCI and TCI as the response variables and the SST anomaly in the Niño 3.4 region as the ENSO proxy. Here we try to answer the following questions from a long and a short-term response, respectively: (1) From a long-term perspective, what is the temporal correlation between VCI and TCI and SST anomalies at the seasonal scale? And (2) from a short-term perspective, what are the impacts of El Niño events on the TDFs based on the MWCA? This analysis is expected to contribute towards a deeper understanding of the vulnerability of TDFs to ENSO and the teleconnection between ENSO and climate variability across the Americas.

2. Methods

2.1. Study sites

This study was conducted in four conservation areas of TDFs in the Americas: Chamela-Cuixmala Biosphere Reserve (CCBR) in Mexico, Parque Estadual da Mata Seca (PEMS) in Brazil, Santa Rosa National Park Environmental Monitoring Super Site (SRNP-EMSS) in Costa Rica, and Tucabaca Valley Municipal Wildlife Reserve (TVMWR) in Bolivia (Fig. 1). These study areas cover different latitudes ranging from 18°15′S to 19°30′N in the Americas. Mean Annual Precipitation (MAP) at the CCBR (763 mm) and PEMS (818 mm) is less, and that at the SRNP-EMSS (1390 mm) and TVMWR (1234 mm) is abundant. These sites have a similar Mean Annual Temperature (MAT), around 25 °C. The start time and end time of the dry season and wet season are different (Table 1). The study sites comprise of secondary TDFS on different levels of ecological succession (Madeira et al., 2009; Janzen, 1998; Portillo-Quintero et al., 2015).

Study areas were chosen for two reasons. In the first place, the dynamics of TDFs in study areas were only affected by environmental factors, such as precipitation and temperature, instead of the effect of human activities. Secondly, study sites distributed along a latitudinal gradient in the Americas are significantly affected by ENSO.

2.2. Remote sensing drought indices

As one of the most widely used drought indexes, the Vegetation Drought Index (VCI) was calculated using the Normalized Difference Vegetation Index (NDVI), which is highly relevant to greenness and vegetation vigor and can be viewed as a proxy of photosynthetic activity (Piao et al., 2020). As a complement, the Temperature Drought Index (TCI) is calculated from Land Surface Temperature (LST), which is closely related to vegetation water stress, soil moisture, and evapotranspiration (Karnieli et al., 2010; Kogan, 1995; Kogan,1997). The monthly VCI and TCI were obtained using the following formula:

$$VCI_{ij} = (NDVI_{ij} - NDVI_{jmin})/(NDVI_{jmax} - NDVI_{jmin})*100 \quad (1)$$

$$TCI_{ij} = (LST_{jmax} - LST_{ij})/(LST_{jmax} - LST_{jmin})*100 \quad (2)$$

Where i describes the i th year, j represents the j th month, and NDVI $_{j\,\max}$ and NDVI $_{j\,\min}$ represent the maximum and minimum NDVI value in the j

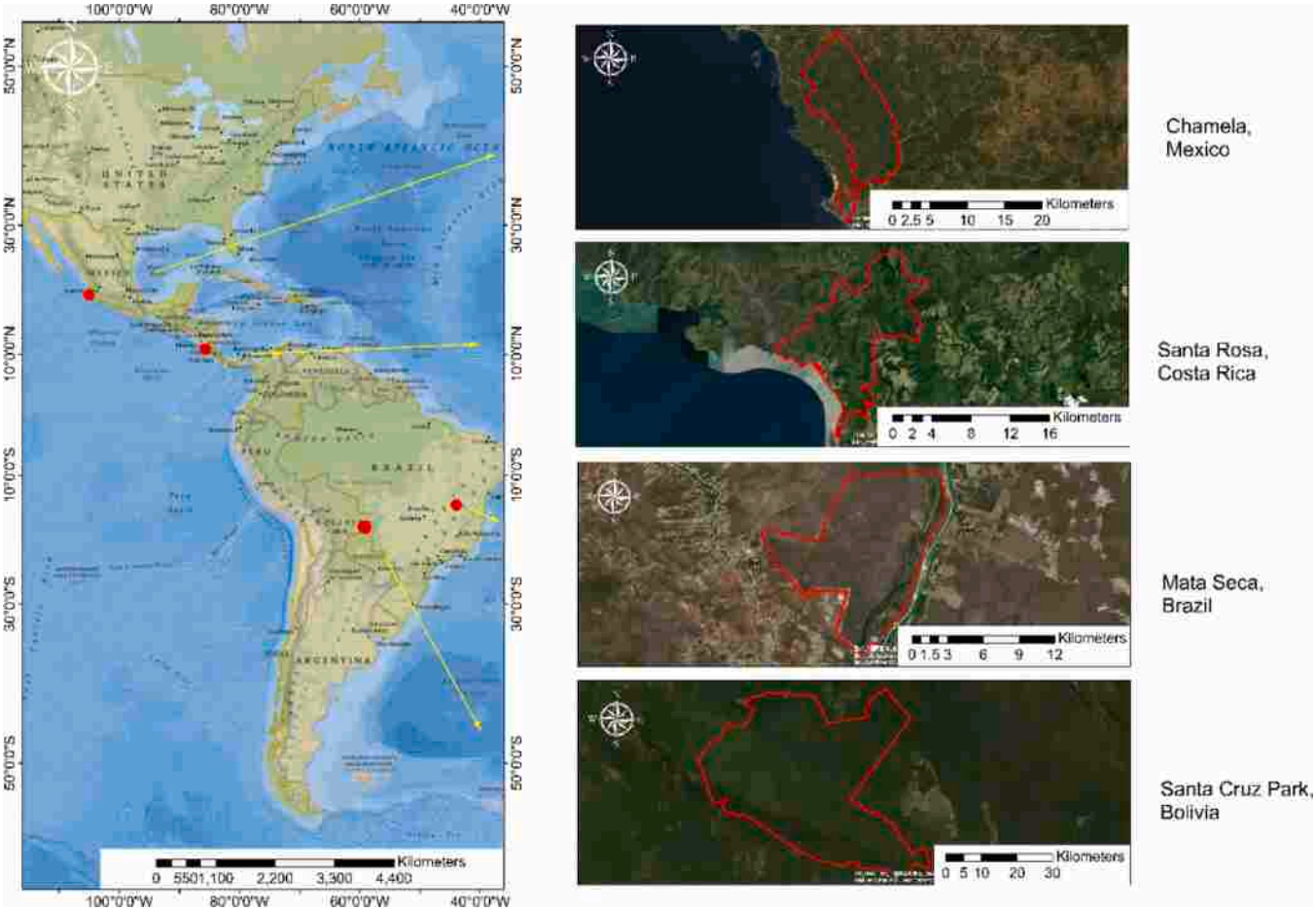

Fig. 1. Study sites in the Americas.

Table 1
Description of the study sites.

Site	Location	Area	Mean annual precipitation (MAP)	Mean annual temperature (MAT)	Dry season	Wet season
CCBR,Mexico	19°30′N,104°58′W	127 km^2	763 mm	24.6°	Nov-May	Jun-Oct
SRNP-EMSS,Costa Rica	10°48′N,85°36′W	108 km^2	1390 mm	26.6°	Dec-Apr	May-Nov
PEMS,Brazil	14°51′S,43°59′W	116 km^2	818 mm	24°	May-Oct	Nov-Apr
TVMWR,Bolivia	18°15′S,59°15′W	1937 km^2	1234 mm	23.9°	Jun-Oct	Nov-May

th month across all the years, respectively. $LST_{j\ max}$ and $LST_{j\ min}$ represent the maximum and minimum LST value in the *j* th month across all the years, respectively. The drought grades can be classified using drought indices (Table 2) (Kogan, 1995; Kogan,1997).

We retrieved the sixteen-day and eight-day Terra Moderate Resolution Imaging Spectroradiometer (MODIS) NDVI (MOD13Q1, collection v006) and LST (MOD11A2, collection v006) products with 250-m and 1-km resolution from March 2000 to March 2017 at reverb echo (http://reverb.echo.nasa.gov/reverb/). These images were re-projected to Universal Transverse Mercator with central zone 16 N° and WGS84. The monthly NDVI and LST were aggregated on a linear weight average of sixteen-day NDVI and eight-day LST after removing the missing data based on the quality file. The weight for each sixteen-day NDVI and eight-day LST imagery is calculated by the number of days belonging to each month divided by the total number of days in the month (Rhee et al., 2010).

Table 2
Classification of remote sensing-based drought indices VCI and TCI.

Name of class	VCI	TCI
Extreme drought	0–10	0–10
Severe drought	10–20	10–20
Moderate drought	20–30	20–30
Mild drought	30–40	30–40
Abnormally dry	40–50	40–50
No drought	50–100	50–100

2.3. ENSO index

The intensity of a specific ENSO event can be described via various ENSO proxies. According to the definition of the National Oceanic and Atmospheric Administration (NOAA), an ENSO warm (cold) event is a phenomenon in the equatorial Pacific Ocean characterized by five consecutive three-month running mean of SST anomalies at or above + 0.5 °C (at or below −0.5 °C) in the Niño 3.4 region (5°S–5°N, 120°W–170°W). ENSO events can be classified as Table 3. As such, El Niño events in 08/2004–03/2005 and 10/2006–02/2007 were classified as weak, those in 07/2002–03/2003 and 08/2009–04/2010 were classified as moderate, and those in 12/2014–06/2016 were classified as very strong (Fig. 2). Each El Niño event was inter-seasonal for four study

Table 3
Classification of ENSO based on SST anomaly.

SST anomaly	Degree	ENSO type
SST $\geq$ 2	Very strong	El Niño
1.5 $\leq$ SST < 2	Strong	El Niño
1.0 < SST $\leq$ 1.5	Moderate	El Niño
0.5 < SST $\leq$ 1.0	Weak	El Niño
−0.5 < SST < 0.5	NaN	Neutral
−1.0 < SST $\leq$ −0.5	Weak	La Niña
−1.5 < SST $\leq$ −1.0	Moderate	La Niña
−2.0 < SST $\leq$ −1.5	Strong	La Niña
SST $\leq$ 2.0	Very strong	La Niña

sites. Therefore, we selected an SST anomaly in the Niño 3.4 region as an ENSO proxy in this study. The monthly SST anomaly can be obtained at (http://www.cpc.ncep.noaa.gov/). The teleconnection between SST anomalies in Niño 3.4 and the terrestrial biosphere has been documented for South America, Southeast Asia, and Africa (Jiménez-Muñoz et al., 2016; Propastin et al., 2010).

2.4. Temporal correlations between VCI and TCI and SST anomalies at the seasonal scale

To understand the teleconnection between ENSO and TDFs from a long-term perspective, the temporal correlations between time series VCI and TCI and SST anomalies in Niño 3.4 were conducted for the dry and wet season, respectively. Time duration and time lag are two key parameters for temporal correlations. Time duration refers to the period of the mean SST anomalies. The value of an SST anomaly in a specific duration is the mean of the monthly SST anomalies in the period. Time lag refers to the interval between the occurrence of the change in an SST anomaly and the change in drought indices. A time duration from 1 to 24 months and a time lag from 0 to 5 months were adopted in the temporal correlation analysis. As a result, there are 144 (24*6) correlation coefficients for the dry season and wet season in each study site (Table 4).

2.5. Moving window correlation analysis (MWCA)

To evaluate the impacts of different El Niño events from March 2000 to March 2017 on TDFs in our study sites, a Moving Window Correlation Analysis (MWCA) approach was used (Erasmi et al., 2009). MWCA is a powerful statistical method used to investigate variations in relationships between two variables in time. The MWCA uses a window with a defined size moving across two time-series data, and the local correlation coefficient is retrieved at each time point. The result of a MWCA is a time series of correlation coefficients with the same dimension as the input of two time-series data. In addition, the result of MWCA varies with the window size (Erasmi et al., 2009).

In this study, MWCA was conducted through two steps. In the first step, the optimal window size was selected by minimizing the four-study-site mean of one-step Root Mean Square Forecast Errors (RMSFEs) (Inoue et al., 2017). The one-step RMSFEs were obtained from monthly VCIs and TCIs as functions of monthly SST anomalies for the window sizes from 5 to 24 months in four sites. Then, eight one-step RMSFEs (2 response variables*4 sites) were averaged for each window size. The optimal window size was selected as the one corresponding to the minimum four-study-site mean of one-step RMSFEs. In the second step, the time-series correlation coefficients and *p*-values were extracted, with VCI and TCI as response variables, and the SST anomaly as an independent variable using MWCA at the optimal window size, imposing different time lags from 0 to 5 months into correlation analysis.

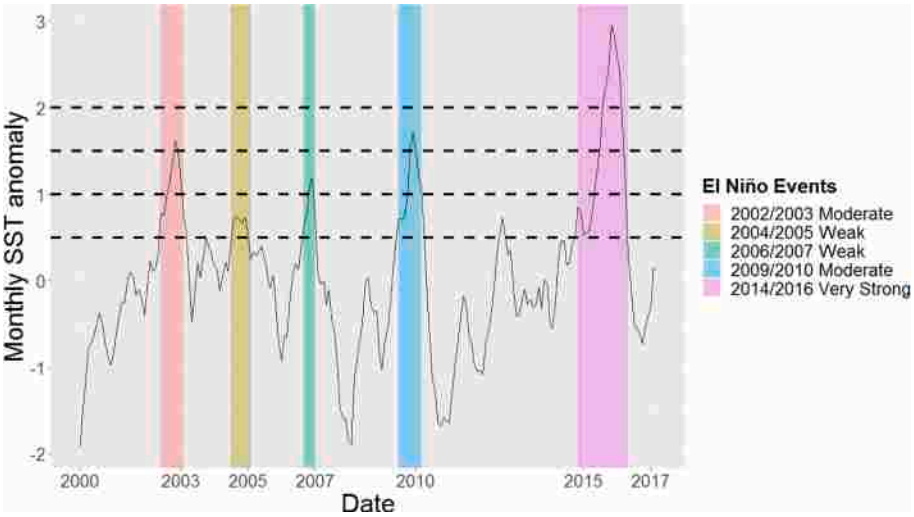

Fig. 2. The monthly SST anomaly in the Niño 3.4 region. The five El Niño events from March 2000 to March 2017 have been highlighted.

Table 4
Temporal patterns (24 time durations * 6 time lags) of correlations between the VCI and TCI and the corresponding multi-scale SST anomalies. The numbers in the cells show the time period for the mean of SST anomalies. Zero corresponds to the current month, one indicates the first previous month, and zero to one shows the period from the current month to the first previous month.

	Duration											
Lag	1	2	3	4	5	6	7	8	9	…	23	24
0	0	0–1	0–2	0–3	0–4	0–5	0–6	0–7	0–8	…	0–22	0–23
1	1	1–2	1–3	1–4	1–5	1–6	1–7	1–8	1–9	…	1–23	1–24
2	2	2–3	2–4	2–5	2–6	2–7	2–8	2–9	2–10	…	2–24	2–25
3	3	3–4	3–5	3–6	3–7	3–8	3–9	3–10	3–11	…	3–25	3–26
4	4	4–5	4–6	4–7	4–8	4–9	4–10	4–11	4–12	…	4–26	4–27
5	5	5–6	5–7	5–8	5–9	5–10	5–11	5–12	5–13	…	5–27	5–28

3. Results

3.1. Monthly variation of NDVI and LST

The phenological characteristics of NDVI and LST were similar for CCBR in Mexico, and SRNP-EMSS in Costa Rica, both of which are located in the northern hemisphere (Fig. 3a–d). PEMS in Brazil and TVMWR in Bolivia are located in the southern hemisphere have similar trends (Fig. 3e–h).

Overall, the median NDVIs in the dry season were lower than those in the wet season, while the median LSTs in the dry season were higher than those in the wet season at the four sites of TDFs (Fig. 3). The NDVIs increased sharply when the wet season arrives. Then they grew slowly until to a high level (about 0.85) in the late wet season. NDVIs decreased slowly when the dry season began and then decreased gradually to a low level (under 0.6) in the late dry season. LSTs in our study sites increased mildly when the dry season started and reached high values (above 308 K) in the dry season. However, the temporal variations for the LSTs at our study sites were not consistent in the wet season, although all of them showed low values (under 302 K) in the wet season. LSTs decreased mildly when the wet season started, and sharply in the second month of the wet season at the CCBR in Mexico, and the SRNP-EMSS in Costa Rica. The sharp decrease occurred in the first month of the wet season at the PEMS in Brazil. The decrease at the TVMWR in Bolivia was gradual during the wet season. The largest variations occurred in the transitional season from dry to wet season in terms of both NDVI and LST at the four sites.

3.2. The temporal relationship between SST anomalies and VCI and TCI

Table 5 shows the teleconnection of the SST anomaly to the VCI and the TCI in the dry and wet seasons for each study site. At the CCBR, Mexico, the VCI in the dry season (November–May) was positively affected by the 3-month average of SST anomalies without a time lag. At the SRNP-EMSS, Costa Rica, the VCI and TCI in the dry season (December–April) were negatively influenced by the 2-month average of SST anomalies with a 5-month lag and 1-month SST anomalies with a 1-month lag; the TCI in the wet season (May–November) was negatively affected by the 3-month average of SST anomalies. At the PEMS, Brazil, the VCI and TCI in the dry season (May–October) were negatively affected by the 3-month average of SST anomalies without a time lag and the 2-month average of SST anomalies without a time lag; the TCI in the wet season (Nov–April) was negatively affected by the 2-month average of SST anomalies without a time lag. At the TVMWR, Bolivia, VCI in the wet season (Nov–May) was positively affected by 21- month averages of SST anomalies without a 5-month lag.

Table 5 illustrates that both the VCI and TCI of SRNP-EMSS, Costa Rica and PEMS, Brazil were negatively affected by SST anomalies in the dry seasons. For the further analysis, Fig. 4 shows the correlation coefficients between the VCI and TCI at the SRNP-EMSS, Costa Rica and PEMS, Brazil and multiple SST anomalies (time durations from 1 to 24 months; time lag from 0 to 5 months). The results illustrate that both the VCI and TCI at the SRNP-EMSS, Costa Rica and the PEMS, Brazil in the dry season were negatively affected by several specific SST anomalies simultaneously. The temporal relationship between SST anomalies and VCIs and TCIs at four sites for both the dry and wet season are in the Supplementary Materials. In particular, the duration of these SST anomalies was less than 13 months. The lag time of these SST anomalies ranged from 0 to 5 months at the SRNP-EMSS, Costa Rica and from 0 and 3 months at the PEMS, Brazil.

3.3. The impacts of El Niño events on TDFs

Figure 5 shows the average of eight one-step RMSFEs obtained from the VCIs and TCIs of four study sites as the function of SST anomalies for different window sizes (5 to 24 months). The result indicated low average one-step RMSFEs occurred at window sizes of 15 and 16 months. Lower RMSFEs can also be observed in larger window sizes, but in these cases, the window sizes exceed the total lengths of El Niño events. Thus, the optimal window size is selected as 15 months, as an odd number is more convenient for the further MWCA.

The results of MWCA revealed that temporal patterns in responses of VCIs and TCIs to SST anomalies were nonstationary (Supplementary Materials). Time lag is a key parameter affecting the MWCA between VCIs and TCIs and SST anomalies. The temporal regions of significantly negative correlations between VCIs and TCIs and SST anomalies illustrated the potential occurrence of El Niño-related drought. The temporal patterns of El Niño periods and the corresponding periods and time lags of El Niño-driven VCI and TCI decrease in four study sites are summarized in Table 6. This reveals the impacts of El Niño events on TDFs over the four study sites from March 2000 to March 2017. Five El Niño events led to 3, 2, 2, 2, and 1 times of VCI decrease, and 2, 1, 2, 1, and 4 times of TCI decrease in four study sites in turn

4. Discussion

4.1. Teleconnection between ENSO and precipitation over TDFs

The predominant factor for the growth of TDFs is water availability (Cao et al., 2016; Castro et al., 2018). Thus, the responses of TDFs to SST anomalies are largely influenced by the teleconnections between ENSO and precipitation. The VCI and TCI are complementary indicators that reflect the precipitation conditions over TDFs (Cao et al., 2016; Castro et al., 2018). As such, ENSO is considered to play a key role in precipitation over TDFs when either the VCI or TCI is significantly influenced by SST anomalies.

The teleconnections differ because ENSO events are unique; and they differ in space, time, and amplitude (Capotondi et al., 2015). SST anomalies across multiple ENSO phases (warm, neutral, and cold phases) can affect precipitation regimes in study sites.

Precipitation patterns at the CCBR, Mexico, SRNP-EMSS, Costa Rica, and PEMS, Brazil were influenced by short-duration SST anomalies. Likewise, the 2014 and 2015 seasonal precipitation amounts in the SRNP-EMSS, Costa Rica represent a 30% and 63% reduction in precipitation due to warm ENSO, respectively (Castro et al., 2018). The precipitation patterns at the TVMWR, Bolivia was affected by the long-duration SST anomalies. In additions, higher SST anomalies across multiple ENSO phases tend to trigger excessive precipitation at the CCBR, Mexico and TVMWR, Bolivia, and less precipitation at the SRNP-EMSS, Costa Rica and the PEMS, Brazil. Our results are consistent with previous studies that the marked interannual variability in precipitation over TDFs in the Santa Rosa, Costa Rica is largely driven by ENSO; and the wettest and driest periods are attributed to La Niña and El Niño (Campos, 2018).

SST anomalies during the ENSO warm phase can lead to droughts in study sites (Table 7). It implies that the intensity of an El Niño event plays an important role in drought conditions for a wide region instead of a specific local region. In other words, stronger El Niño events may lead to severe droughts in more regions across TDFs, but there is no direct relationship between the intensity of an individual El Niño event and the precipitation condition in each study site. The climate conditions at SRNP-EMSS, Costa Rica, CCBR, Mexico and TVMWR, Bolivia are sensitive to El Niño events. The short-term teleconnection between SST anomalies during the ENSO warm phase and precipitation was weak for the PEMS, Brazil. But long-term teleconnection between SST anomalies across multiple ENSO phases (warm, neutral, and cold) and precipitation was significant. It revealed that the precipitation over the PEMS, Brazil should be strongly influenced by the ENSO cold phase (La Niña) instead of the warm phase (El Niño).

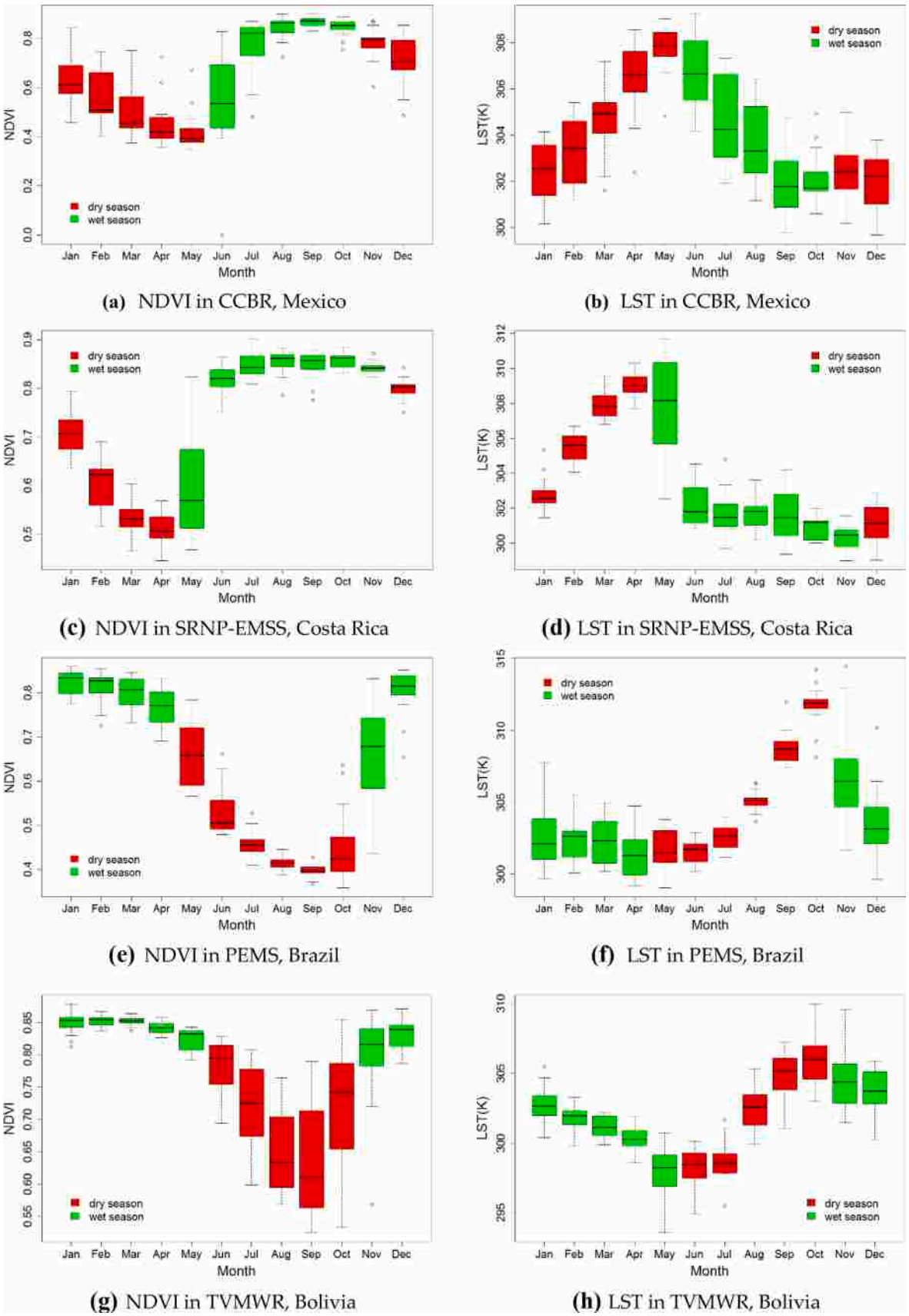

Fig. 3. Monthly NDVI and LST distributions across the latitudinal gradient of TDFs in the Americas from March 2000 to March 2017.

Table 5
The extremums of temporal correlations between the VCI and TCI and SST anomalies in the dry and wet season across the latitudinal gradients of TDFs. The extremum (Rmax (duration, lag) or Rmin (duration, lag)) for the dry season and wet season in each study site was selected from 144 (24 duration*6 lag) correlation coefficients. If the maximum absolutes are obtained by the positive correlations, the extremums are chosen as the maximum values; if the maximum absolutes are obtained by negative correlations, the extremums are chosen as the minimum values. The stars indicate significant correlations with a p-value less than 0.05. No stars indicate that p-values greater than 0.05. Bold fonts indicate the significant correlations.

Sites	VCI-SST anomaly correlation		TCI-SST anomaly correlation	
	Dry season	Wet season	Dry season	Wet season
CCBR, Mexico	**$R_{max}(3,0)$ = 0.34***	$R_{min}(3,5)$ = -0.13	$R_{min}(24,5)$ = -0.14	$R_{min}(5,3)$ = -0.17
SRNP-EMSS, Costa Rica	**$R_{min}(2,5)$ = -0.42***	$R_{max}(24,5)$ = 0.14	**$R_{min}(1,1)$ = -0.58***	**$R_{min}(3,0)$ = -0.32***
PEMS, Brazil	**$R_{min}(3,0)$ = -0.38***	$R_{min}(14,0)$ = -0.27	**$R_{min}(2,0)$ = -0.45***	**$R_{min}(2,0)$ = -0.36***
TVMWR, Bolivia	$R_{max}(1,0)$ = 0.20	**$R_{max}(21,5)$ = 0.35***	$R_{max}(24,5)$ = 0.12	$R_{max}(16,5)$ = 0.27

4.2. Teleconnection between ENSO and the productivity of TDFs

The primary response of forests to climate anomalies is a decline in productivity (Dale et al., 2001). One of the mainstream approaches to estimate GPP globally is based on the light-use efficiency (LUE) concept (Running et al., 2004). The productivity of TDFs is considered to be affected by ENSO when both VCI and TCI have significant correlations with specific SST anomalies (Supplementary Materials).

SST anomalies across multiple ENSO phases (warm, neutral, and cold phases) potentially affect the GPP of TDFs in the dry season rather than wet season. One of the reasons is that the abundant precipitation in the wet season which can mitigate the effect of climate anomalies (Zou et al., 2020a; b). The GPP at CCBR, Mexico and TVMWR, Bolivia in the dry season were not significantly influenced by SST anomalies. This is because the TCI at CCBR, Mexico and both the VCI and TCI at TVMWR, Bolivia in the dry season did not respond to the specific precipitation pattern related to ENSO. The GPP at the SRNP-EMSS, Costa Rica and the PEMS, Brazil in the dry season were significantly influenced by SST anomalies (Fig. 4). This result is consistent with our previous work that the GPP of TDFs at the SRNP-EMSS are sensitive to precipitation in the dry season (Zou et al., 2020b).

The GPP of TDFs in SRNP-EMSS, Costa Rica are the most sensitive to El Niño events, followed by those in CCBR, Mexico (Table 8). It implies that the teleconnections between SST anomalies during ENSO warm phases and climate conditions are strong, and TDFs are sensitive to El Niño-driven droughts. Previous study indicated the GPP of TDFs at SRNP-EMSS was reduced by 13% and 42% due to El Niño-driven

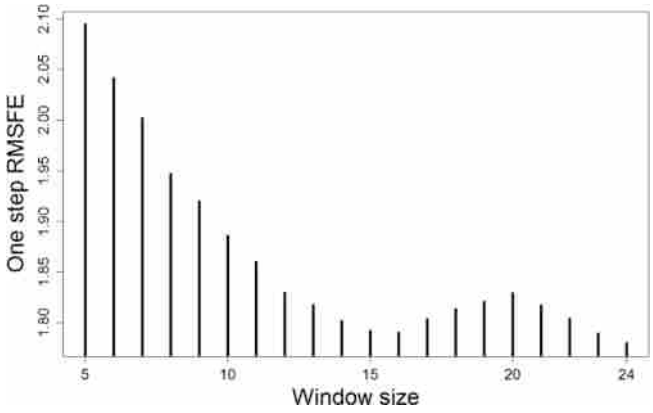

Fig. 5. The mean of 8 one-step RMSFEs derived from VCIs and TCIs of four study sites as the function of the SST anomalies, using different window sizes (5 to 24 months).

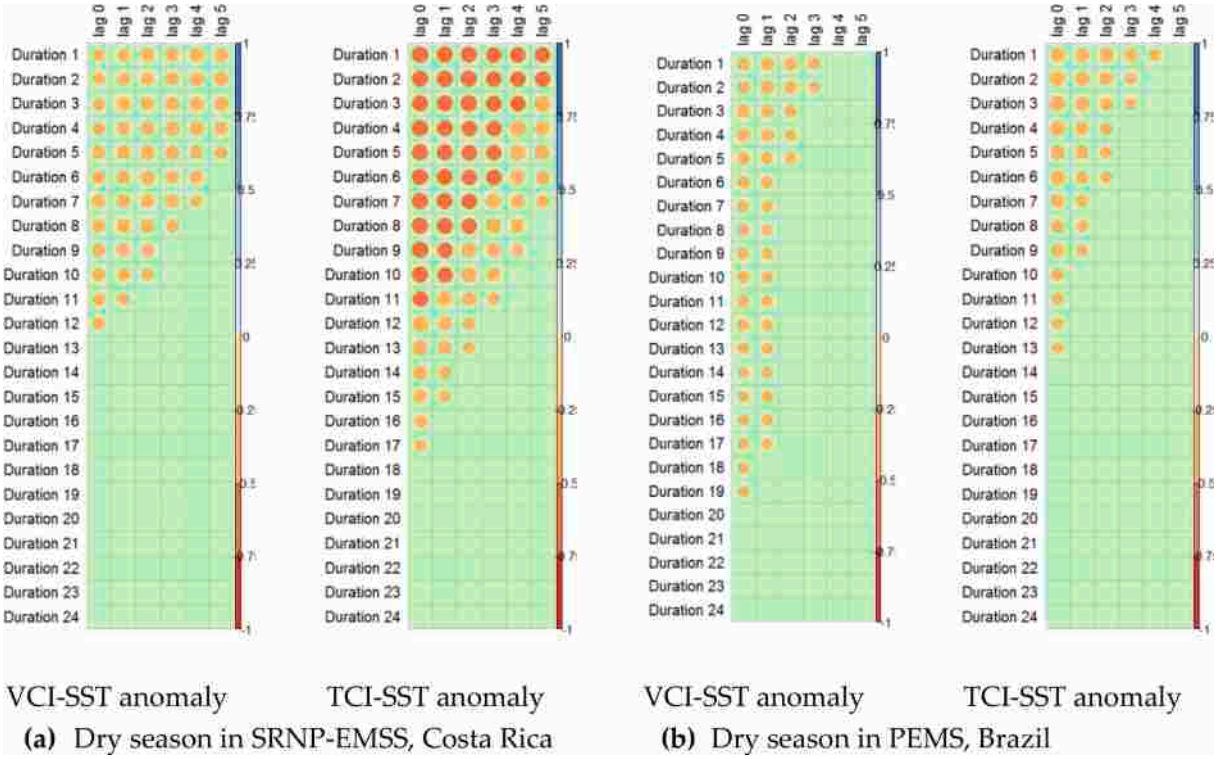

Fig. 4. The response of TDFs to SST anomalies from a long-term perspective in SRNP-ENSS and PEMS in the dry season. Orange circles represents negative correlations (significance level = 0.05). The blank gaps showed no significant correlations. The circle sizes are corresponding to the absolute values of correlation coefficients. (For interpretation of the references to colour in this figure legend, the reader is referred to the web version of this article.)

Table 6
El Niño periods and corresponding periods and time lags of El Niño-driven VCI and TCI decrease. The periods of El Niño-driven VCI and TCI decrease are the intersections of three periods: (1) the periods between El Niño outbreaks and El Niño ending plus the maximum lag time (5 months), (2) the periods in which the results of MWCA based-VCIs and TCIs and SST anomaly were negatively significant, and (3) the periods in which VCIs and TCIs are less than 50 (threshold for drought).

El Niño episode	El Niño-drivenVCI decrease (CCBR,Mexico)	El Niño-driven TCI decrease (CCBR, Mexico)	El Niño-driven VCI decrease (SRNP-EMSS, Costa Rica)	El Niño-driven TCI decrease(SRNP-EMSS,Costa Rica)	El Niño-drivenVCI decrease (PEMS,Brazil)	El Niño-drivenTCI decrease(PEMS, Brazil)	El Niño-drivenVCI decrease (TVMWR, Bolivia)	El Niño-drivenTCI decrease (TVMWR,Bolivia)
07/2002–03/2003(9 month) Moderate	02/2003–06/2003 Time lag = 4	02/2003–05/2003 Time lag = 3	01/2003–03/2003 Time lag = 2	02/2003–04/2003 Time lag = 1	None	None	07/2002–12/2002 Time lag = 0	None
08/2004–03/2005 (8 month) Weak	10/2004–05/2005 Time lag = 5	09/2004–04/2005 Time lag = 4	12/2004–07/2005 Time lag = 5	None	None	None	None	None
10/2006–02/2007(5 month) Weak	01/2007–07/2007 Time lag = 5	01/2007–06/2007 Time lag = 4	01/2007–03/2007 Time lag = 3	10/2006,01/2007/–02/2007 Time lag = 2	None	None	None	None
08/2009–04/2010 (9 month) Moderate	None	None	08/2009 Time lag = 2	09/2009–04/2010 Time lag = 0	None	None	09/2015 Time lag = 5	None
12/2014–06/2016 (19 month) Very strong	None	08/2015–09/2015 Time lag = 211/2015 Time lag = 5	03/2015 Time lag = 501/2016–04/2016 Time lag = 2	03/2015–08/2015,12/2015–04/2016Time lag = 006/2016-10/2016Time lag = 2	None	01/2015–06/2015 Time lag = 212/2015–08/2016Time lag = 1	None	04/2016–05/2016Time lag = 207/201608/2016Time lag = 1

Table 7
Five El Niño events and corresponding El Niño-driven droughts in each study site. One indicates that the El Niño event trigger drought. Zero indicates the El Niño event does not trigger drought. Total El Niño percentage is the total times of occurrence of droughts in each site divided by the total times of El Niño events. Total sites percentage is the total times of occurrence of droughts in El Niño event divided by the total number of study sites.

El Niño episode	El Niño-driven drought (CCBR, Mexico)	El Niño-driven drought (SRNP-EMSS, Costa Rica)	El Niño-driven drought (PEMS, Brazil)	El Niño-driven drought (TVMWR, Bolivia)	Total sites percentage
07/2002–03/2003 (9 month) Moderate	1	1	0	1	75%
08/2004–03/2005 (8 month) Weak	1	1	0	0	50%
10/2006–02/2007 (5 month) Weak	1	1	0	0	50%
08/2009–04/2010 (9 month) Moderate	0	1	0	1	50%
12/2014–06/2016 (19 month)Very strong	1	1	1	1	100%
Total El Niño percentage	80%	100%	20%	60%	65%

droughts in 2014 and 2015 (Castro et al., 2018). However, the GPP of TDFs over PEMS, Brazil and TVMWR, Bolivia is resistant to El Niño events. Although the ocean–atmosphere coupling for TVMWR and Bolivia during El Niño events is strong, the TDFs are resistant to El Niño-driven droughts due to their biophysical characteristics, which can be reflected by higher greenness and lower surface temperature (Fig. 3(g) and (h)). The weak ocean–atmosphere coupling during ENSO warm phase for TVMWR, Brazil is the reason for the resistance of TDFs to El Niño events. It also implies that the primary response of TDFs to SST anomalies does not depend on the intensity of El Niño events for each site and the whole region. This is due to two reasons. First, the effects of SST anomalies on precipitation in a specific site are not consistent between El Niño events. On the other hand, TDFs have some resistance to the El Niño driven drought.

4.3. Comparison of VCI and TCI in response to climate condition

The relationship between the VCI and TCI and SST anomalies can indirectly reflect how greenness and canopy surface temperature respond to climate conditions (Zou et al., 2020a). The capacities of greenness and canopy surface temperature over TDFs reflecting climate conditions vary with season and site. Greenness is sensitive to precipitation at the CCBR, Mexico in the dry season and at the TVMWR, Bolivia in the wet season. On the other hand, although both greenness and evapotranspiration are good indicators to reflect the climate condition at the SRNP-EMSS, Costa Rica and the PEMS, Brazil in the dry and wet seasons, the canopy surface temperature is more sensitive to precipitation than greenness. Our results agreed with previous studies that greenness is more sensitive for drought monitoring in the dry and growing seasons over TDFs, but canopy surface temperature performed better in the wet and senescence seasons (Zou et al., 2020a). Greenness and evapotranspiration at TDFs are complementary biophysical and state properties which can reflect the intensity of El Niño-driven droughts. The shorter time lags of TCI-SST anomalies for the CCBR, Mexico and the SRNP-EMSS, Costa Rica hints that evapotranspiration has a stronger capacity to capture the onset of El Niño-driven droughts at the CCBR, Mexico and SRNP-EMSS, Costa Rica, where El Niño tends to trigger severe impacts on the GPP of TDFs.

Table 8
Five El Niño events and corresponding El Niño-driven productivity declines in each study site. One indicates that the El Niño event trigger drought. Zero indicates the El Niño event does not trigger productivity decline. Total El Niño percentage is the total times of occurrence of productivity declines in each site divided by the total times of El Niño events. Total sites percentage is the total times of occurrence of productivity declines in El Niño event divided by the total number of study sites.

El Niño episode	El Niño-driven productivity decline (CCBR, Mexico)	El Niño-drivenproductivity decline (SRNP-EMSS, Costa Rica)	El Niño-driven productivity decline (PEMS, Brazil)	El Niño-driven productivity decline (TVMWR, Bolivia)	Total percentage
07/2002–03/2003 (9 month) Moderate	1	1	0	0	50%
08/2004–03/2005 (8 month) Weak	1	0	0	0	25%
10/2006–02/2007 (5 month) Weak	1	1	0	0	50%
08/2009–04/2010 (9 month) Moderate	0	1	0	0	25%
12/2014–06/2016 (19 month) Very strong	0	1	0	0	25%
Total percentage	60%	80%	0%	0%	35%

5. Conclusions

The relationship between SST anomalies in the Pacific Niño 3.4 region, and remote sensing drought indices is key to understand how ENSO influences climatology, and therefore the GPP of TDFs in the Americas. We found stronger El Niño events tend to cause severe droughts in more regions. However, there is no evidence of direct relationship between the intensity of an individual El Niño event and the precipitation condition in each study site. Except for their teleconnections, the biophysical characteristics and seasonality can influence the response of ENSO on the GPP of TDFs. We also found that ecosystem level greenness and canopy surface temperature are complementary indicators to better understand climatic conditions at TDFs in the Americas.

There are several limitations that should be considered in the future. Firstly, although we implemented the spatial analysis in the study sites (Supplementary Materials), the analysis for spatial variation is the weakness due to choosing the natural reserves as our study sites instead of the whole TDFs in the world. This is because our method could not take the effect of land change due to the deforestation, degradation, and wildfire into account. Secondly, to reduce the uncertainties, accurate estimate of the GPP is necessary. Multiple data resources (remote sensing, in-situ, and modelling) should be integrated to estimate GPP for TDFs. In the future work, we will improve our method for removing impacts due to land use and combine multiple data source to estimate GPP, which will help better understand the relationship between biophysical and state parameters of TDFs and ENSO temporally and spatially.

This work has two implications. In the first place, the vulnerability and resistance of TDFs to teleconnection varies with seasonal timing. Secondly, the impacts of ENSO-driven drought on TDFs depend on the intensity and of ENSO, as well as their biophysical properties and phenology. Our results may facilitate the development of management and protection policies of TDFs, since they identify the main drivers influencing the productivity of TDFs.

CRediT authorship contribution statement

Lidong Zou: Conceptualization, Methodology, Software, Formal analysis, Writing – original draft. **Sen Cao:** Data curation, Writing – review & editing. **Zaichun Zhu:** Conceptualization, Supervision, Funding acquisition, Writing – review & editing. **Arturo Sanchez-Azofeifa:** Conceptualization, Supervision, Writing – review & editing.

Declaration of Competing Interest

The authors declare that they have no known competing financial interests or personal relationships that could have appeared to influence the work reported in this paper.

Acknowledgments

This research was funded by the Shenzhen Fundamental Research Program (GXWD20201231165807007-20200814213435001). We would also like to thank the support from Prof. Ralf Ludwig at the University of Munich, Prof. Benoit Rivard and Dr. Kayla Stan at the University of Alberta.

Appendix A. Supplementary data

Supplementary data to this article can be found online at https://doi.org/10.1016/j.ecolind.2021.108390.

References

Allen, C.D., Macalady, A.K., Chenchouni, H., Bachelet, D., McDowell, N., Vennetier, M., Hogg, E.T., 2010. A global overview of drought and heat-induced tree mortality reveals emerging climate change risks for forests. For. Ecol. Manag. 259, 660–684.

Anyamba, A., Tucker, C.J., Mahoney, R., 2002. From El Niño to La Niña: Vegetation response patterns over east and southern Africa during the 1997–2000 period. J. Clim. 15, 3096–3103.

Bajgain, R., Xiao, X., Wagle, P., Basara, J., Zhou, Y., 2015. Sensitivity analysis of vegetation indices to drought over two tallgrass prairie sites. J. Photogramm. Remote Sens. 108, 151–160.

Boyd, D.S., Phipps, P.C., Foody, G.M., Walsh, R., 2002. Exploring the utility of NOAA AVHRR middle infrared reflectance to monitor the impacts of ENSO-induced drought stress on Sabah rainforests. Int. J. Remote Sens. 23, 5141–5147.

Browne, L., Markesteijn, L., Engelbrecht, B.M., Jones, F.A., Lewis, O.T., Manzané-Pinzón, E., Comita, L.S., 2021. Increased mortality of tropical tree seedlings during the extreme 2015–16 El Niño. Glob. Chang. Biol. 27, 5043–5053.

Campos, F.A. (2018) A Synthesis of Long-Term Environmental Change in Santa Rosa, Costa Rica. In Primate Life Histories, Sex Roles, and Adaptability. Developments in Primatology: Progress and Prospects; Kalbitzer, U., Jack K., Eds.; Springer, Cham: Switzerland,2018; pp. 331-358.

Cai, W., Santoso, A., Collins, M., Dewitte, B., Karamperidou, C., Kug, J., Zhong, W., 2021. Changing El Niño-Southern Oscillation in a warming climate. Nat. Rev. Earth Environ. 2, 628–644.

Cao, S., Sanchez-Azofeifa, G.A., Duran, S.M., Calvo-Rodriguez, S., 2016. Estimation of aboveground net primary productivity in secondary tropical dry forests using the Carnegie–Ames–Stanford approach (CASA) model. Environ. Res. Lett. 11, 075004.

Capotondi, A., Wittenberg, A.T., Newman, M., Di Lorenzo, Braconnot, P., Cole, J., Dewitte, B., Giese, B., Guilyardi, E. **2015.** Understanding ENSO diversity. *Bull. Am. Meteorol. Soc*. 96, 921-938.

Castro, S.M., Sanchez-Azofeifa, G.A., Sato, H., 2018. Effect of drought on productivity in a Costa Rican tropical dry forest. Environ. Res. Lett. 13, 045001.

Chadwick, W.W., Paduan, J.B., Clague, D.A., Dreyer, B.M., Merle, S.G., Bobbitt, A.M., Nooner, S.L., 2016. Voluminous eruption from a zoned magma body after an increase in supply rate at axial seamount. Geophys. Res. Lett. 43, 12063–12070.

Dale, V.H., Joyce, L.A., McNulty, S., Neilson, R.P., Ayres, M.P., Flannigan, M.D., Peterson, C.J., 2001. Climate change and forest disturbances: Climate change can affect forests by altering the frequency, intensity, duration, and timing of fire, drought, introduced species, insect and pathogen outbreaks, hurricanes, windstorms, ice storms, or landslides. Bioscience. 51, 723–734.

Doughty, R., Xiao, X., Qin, Y., Wu, X., Zhang, Y., Moore III, B., 2021. Small anomalies in dry-season greenness and chlorophyll fluorescence for Amazon moist tropical forests during El Niño and La Niña. Remote Sens. Environ. 253, 112196.

Erasmi, S., Propastin, P., Kappas, M., Panferov, O., 2009. Spatial patterns of NDVI variation over Indonesia and their relationship to ENSO warm events during the period 1982–2006. J. Clim. 22, 6612–6623.

Fahad, S., Sonmez, O., Saud, S., Wang, D., Wu, C., Adnan, M., Turan, V. (Eds.), 2021a. Climate Change and Plants: Biodiversity, Growth and Interactions. CRC Press.

Fahad, S., Sonmez, O., Saud, S., Wang, D., Wu, C., Adnan, M., Turan, V. (Eds.). Plant Growth Regulators for Climate-Smart Agriculture. CRC Press. **2021c**.

Fahad, S., Ullah, A., Ali, U., Ali, E., Saud, S., Hakeem, K.R., Arif, M., 2019. Drought tolerance in plants role of phytohormones and scavenging system of ROS. In: Plant Tolerance to Environmental Stress. CRC Press, pp. 103–114.

Gregory, N., Ewers, R.M., Chung, A.Y.C., Cator, L.J., 2019. Niño drought and tropical forest conversion synergistically determine mosquito development rate. Environ. Res. Lett. 14 (3), 035003. https://doi.org/10.1088/1748-9326/ab0036.

Holmgren, M., Scheffer, M., Ezcurra, E., Gutiérrez, J.R., Mohren, G.M.E., 2001. Niño effects on the dynamics of terrestrial ecosystems. Trends Ecol. Evol. 16, 89–94.

Inoue, A., Jin, L., Rossi, B., 2017. Rolling window selection for out-of-sample forecasting with time-varying parameters. J. Econom. 196, 55–67.

Janzen, D.H., 1998. Management of habitat fragments in a tropical dry forest: growth. Ann. Mo. Bot. Gard. 75, 105–116.

Jiménez-Muñoz, J., Mattar, C., Barichivich, J., Santamaría-Artigas, A., Takahashi, K., Malhi, Y., Van Der Schrier, G., 2016. Record-breaking warming and extreme drought in the Amazon rainforest during the course of El Niño 2015–2016. Sci. Rep. 6, 1–7.

Juan, C.J., Jose, A., Lincoln, M., Juan, C.S., Ken, T., Samantha, F., Matthew, C. 2021. The role of ENSO flavours and TNA on recent droughts over Amazon forests and the Northeast Brazil region. Int. J. Climatol. 41, 3761-3780.

Karnieli, A., Agam, N., Pinker, R.T., Anderson, M., Imhoff, M.L., Gutman, G.G., Goldberg, A., 2010. Use of NDVI and land surface temperature for drought assessment: merits and limitations. J. Clim. 23, 618–633.

Kogan, F.N., 1995. Application of vegetation index and brightness temperature for drought detection. Adv. Space Res. 15, 91–100.

Kogan, F.N., 1997. Global drought watch from space. Bull. Am. Meteorol. Soc. 78, 621–636.

Lopezaraiza-Mikel, M., Quesada, M., Álvarez-Añorve, M., Ávila-Cabadilla, L., Martén-Rodríguez, S., Calvo-Alvarado, J. **2013.** Phenological patterns of tropical dry forests along latitudinal and successional gradients in the Neotropics. Phenological patterns of tropical dry forests along latitudinal and successional gradients in the Neotropics. In Tropical dry forests in the Americas; Sanchez-Azofeifa, A, Powers, J.S., Fernandes, G.W., Quesada.M, Eds.; CRC Press, pp. 119-146.

Madeira, B.G., Espírito-Santo, M.M., Neto, S.D., Nunes, Y.R., Sanchez-Azofeifa, A., Fernandes, G.W., Quesada, M., 2009. Changes in tree and liana communities along a successional gradient in a tropical dry forest in South-Eastern Brazil. J. Plant Ecol. 201, 291–304.

Marengo, J.A., Tomasella, J., Alves, L.M., Soares, W.R., Rodriguez, D.A., 2011. The drought of 2010 in the context of historical droughts in the Amazon region. Geophys. Res. Lett. 38.

Mennis, J., 2001. Exploring relationships between ENSO and vegetation vigour in the South-East USA using AVHRR data. Int. J. Remote Sens. 22, 3077–3092.

Nagai, S., Ichii, K., Morimoto, H., 2007. Interannual variations in vegetation activities and climate variability caused by ENSO in tropical rainforests. Int. J. Remote Sens. 28, 1285–1297.

Piao, S., Wang, X., Park, T., Chen, C., Lian, X., He, Y., Myneni, R., 2020. Characteristics, drivers and feedbacks of global greening. Nat. Rev. Earth Environ. 1, 14–27.

Portillo-Quintero, C., Sanchez-Azofeifa, A., Calvo-Alvarado, J., Quesada, M., do Espirito Santo, M.M., 2015. The role of tropical dry forests for biodiversity, carbon and water conservation in the Neotropics: Lessons learned and opportunities for its sustainable management. Reg. Environ. Chang. 15, 1039–1049.

Propastin, P., Fotso, L., Kappas, M., 2010. Assessment of vegetation vulnerability to ENSO warm events over Africa. Int. J. Appl. Earth Obs. Geoinf. 12, S83–S89.

Rhee, J., Im, J., Carbone, G.J., 2010. Monitoring agricultural drought for arid and humid regions using multi-sensor remote sensing data. Remote Sens. Environ. 114, 2875–2887.

Running, S.W., Nemani, R.R., Heinsch, F.A., Zhao, M., Reeves, M., Hashimoto, H., 2004. A continuous satellite-derived measure of global terrestrial primary production. Bioscience 54, 547–560.

Sanchez-Azofeifa, G.A., Quesada, M., Rodríguez, J.P., Nassar, J.M., Stoner, K.E., Castillo, A., Cuevas-Reyes, P., 2005. Research priorities for Neotropical dry forests. Biotropica. 37, 477–485.

Sun, H., Zhao, X., Chen, Y., Gong, A., Yang, J., 2013. A new agricultural drought monitoring index combining MODIS NDWI and day–night land surface temperatures: a case study in China. Int. J. Remote Sens. 34, 8986–9001.

Wan Mohd Jaafar, W.S., Abdul Maulud, K.N., Muhmad Kamarulzaman, A.M., Raihan, A., Md Sah, S., Ahmad, A., Saad, S.N.M., Mohd Azmi, A.T., Jusoh Syukri, N.K.A., Razzaq Khan, W. **2020**. The influence of deforestation on land surface temperature—A case study of Perak and Kedah, Malaysia. *Forests* 11, 670.

Zhang, L., Jiao, W., Zhang, H., Huang, C., Tong, Q. (2017) Studying drought phenomena in the continental United States in 2011 and 2012 using various drought indices. Remote Sens. Environ. 190, 96–106.

Zou, L., Cao, S., Sanchez-Azofeifa, A., 2020a. Evaluating the utility of various drought indices to monitor meteorological drought in tropical dry forests. Int. J. Biometeorol. 64, 701–711.

Zou, L., Cao, S., Zhao, A., Sanchez-Azofeifa, A., 2020b. Assessing the temporal response of tropical dry forests to meteorological drought. Remote Sens. 12 (14), 2341. https://doi.org/10.3390/rs12142341.